



# Modelling the Effect of Variable Viscosity on Unsteady Couette Flow of Nanofluids with Convective Cooling

A. O. Ali<sup>1†</sup> and O. D. Makinde<sup>2</sup>

<sup>1</sup> Nelson Mandela African Institution of Science and Technology (NM-AIST), Arusha, Tanzania.  
<sup>2</sup> Faculty of Military Science, Stellenbosch University, Private Bag X2, Saldanha 7395, South Africa.

†Corresponding Author Email: [alia@nm-aist.ac.tz](mailto:alia@nm-aist.ac.tz)

(Received May 4, 2014; accepted October 1, 2014)

## ABSTRACT

This paper investigates numerically the effects of variable viscosity on unsteady generalized Couette flow of a water base nanofluid with convective cooling at the moving surface. The Buongiorno model utilized for the nanofluid incorporates the effects of Brownian motion and thermophoresis. The nonlinear governing equations of continuity, momentum, energy and nanoparticles concentration are tackled numerically using a semi discretization finite difference method together with Runge-Kutta Fehlberg integration scheme. Numerical results for velocity, temperature, and nanoparticles concentration profiles together with skin friction and Nusselt number are obtained graphically and discussed quantitatively.

**Keywords:** Couette flow; Nanofluids; Heat transfer; Variable viscosity; Convective cooling.

## NOMENCLATURE

$A$	pressure gradient parameter	$T_0$	initial temperature
$a$	width of the channel	$T_a$	ambient temperature
$Bi$	Biot number	$\bar{t}$	time
$C_p$	specific heat capacity	$t$	dimensionless time
$c_f$	skin friction	$U$	upper plate uniform velocity
$D_B$	Brownian diffusion coefficient	$u$	nanofluid velocity in $x$ -direction
$D_T$	thermophoretic coefficient	$W$	dimensionless velocity
$Ec$	Eckert number		
$H$	dimensionless particle volume fraction	$\tau$	ratio of solid particle specific heat capacity with fluid specific heat capacity
$h$	heat transfer coefficient	$\beta$	variable viscosity parameter
$k_f$	thermal conductivity of nanofluid	$\eta$	dimensionless $x$ -axis
$\bar{P}$	dimensionless pressure	$\alpha_f$	thermal diffusivity of nanofluid
$m$	viscosity variation parameter	$\mu_f$	viscosity of nanofluid
$Nb$	Brownian motion parameter	$\mu_0$	viscosity at initial temperature $T_0$
$Nu$	Nusselt number	$\theta$	dimensionless temperature
$P$	nanofluid pressure	$\phi$	nanoparticle concentration
$Pr$	Prandtl number	$\rho_f$	density of nanofluid
$q_w$	heat flux at the moving plate	$\nu_f$	kinematic viscosity of nanofluid
$Re_f$	Local Reynolds number	$\phi_0$	initial nanoparticle concentration
$Sc$	Schmidt number	$\tau_w$	shear stress at the moving plate
$T$	temperature of nanofluid		

## 1. INTRODUCTION

Convective heat transfer using nanofluids has received considerable attention in recent decades (Wang and Mujumdar 2007). This is due to their diverse application in many industrial and engineering applications. Among the area where nanofluids are utilized are in heat exchange systems

in electronics devices, power generation, automobile engines, welding equipment and cooling of nuclear reactors (Motsumi and Makinde 2012; Sheikholeslami and Ganji 2014). The term nanofluid coined by Choi (1995), refers to stable suspension of tiny particles (less than 100nm) in a base fluid. The first vital step in experimental studies which involve nanofluids is its preparation. During preparation, the fundamental requirements

that nanofluids should be in accordance with are stable and evenly distributed suspension, no chemical change within the nanofluid and negligible particles agglomeration. One of the methods of nanofluids preparation involves production of nanoparticles using gas condensation, before spreading them into the base fluid. Ultrasound is mostly employed in this method to produce sufficient and stable blend (Wang et al. 1999; Kiblinki et al. 2002). Another process involves evaporation of nanoparticles in oil substrate. The particles then grew onto the oil substrate in the base fluid. This process is referred as vacuum evaporation on running oil substrate (VEROS) (Buongiorno 2006). Particles can be produced in different structures and sizes, ultra-fine particles suspended in a base fluid greatly enhance the performance of transport and heat transfer properties of the systems (Xuan and Roetzel 2000). Choi et al. (2001) reported that, compared with other nano-structured materials suspended in base fluids, nanotubes demonstrate anomalously greatest heat transfer enhancement, greater than the theoretical predictions, and exhibit nonlinear relationship with nanotubes loadings, widening up the range of nanotubes applications.

In practical applications the flow of nanofluids are commonly associated with mechanical systems. One of the common flows in fluid dynamics which occur in mechanical systems is Couette flow, a shear flow between two parallel surfaces, one moving tangentially relative to the other. The Couette flow occurs in fluid machineries involving moving parts and is essential for hydrodynamic lubrications (Yasutomi et al., 1984; Gao and Lu, 2013).

Several models have been suggested to describe the effects of nanofluids on heat and mass transfer enhancement. Maiga et al. (2005) numerically investigated laminar forced convection flow of nanofluids (water- $\text{Al}_2\text{O}_3$  and ethylene glycol- $\text{Al}_2\text{O}_3$ ) for homogeneously heated tube. Results revealed that nanofluids demonstrate considerable heat transfer enhancement, which is proportional to the particle concentration. Although it generated wall shear stress proportional to the particle volume fraction with more pronounced adverse effects, ethylene glycol- $\text{Al}_2\text{O}_3$  has shown a better heat transfer performance than water- $\text{Al}_2\text{O}_3$ . Sheikholeslami et al. (2013) used the lattice Boltzmann method (LBM) to examine free convection of nanofluids. The nanofluids ( $\text{TiO}_2$ , Ag, Cu and  $\text{Al}_2\text{O}_3$ ) were filled in the space between the cold outer square and heated inner circular cylinder. Numerical solutions using LBM demonstrated an excellent agreement with those obtained from other numerical methods. They also reported that copper nanoparticles exhibited the highest heat transfer enhancement. Along that line, Makinde (2004) investigated the combined effects of viscous dissipation and Newtonian heating on boundary-layer flow over a flat plate using water based nanofluids containing copper (Cu), alumina ( $\text{Al}_2\text{O}_3$ ), and titania ( $\text{TiO}_2$ ) for various nanoparticle volume fractions. Cu-water nanofluid demonstrated

higher heat transfer performance than that of  $\text{Al}_2\text{O}_3$ -water and  $\text{TiO}_2$ -water nanofluids, which increase with the increase in nanoparticle volume fractions.

Couette flow plays an essential role in heat and mass transfer systems. Dong and Johnson (2005) compared experimental investigation of instabilities of a channel Couette flow composed of two layers of immiscible fluids. They reported that experimental results well matched with the theoretical predictions. Accordingly, Chinyoka and Makinde (2011) incorporated the exothermic chemical kinetics and asymmetric convective heat exchanges with the ambient temperatures at the channel surfaces to analyze the unsteady generalized Couette flow and heat transfer in a reactive variable viscosity third grade liquid. In contrast, Ahmad (2012) analyzed Couette flow by introducing arbitrary non-uniform magnetic field. Other researchers who presented works on Couette flow and convective heat transfer include Nag et al. (1979), Gireesha et al. (2012) and Das et al. (2009), Hatami et al. (2014), Kuznetsov and Nield (2014), Jamaï et al. (2014), among many others.

More comprehensive reviews with detailed discussions on nanofluids convective transport are presented in Trisaksri and Wongwises (2007), Wang and Mujumdar (2007), Eastman et al. (2004) and Kakac and Pramuanjaroenkij (2009), to list just a few.

Meanwhile, Makinde and Aziz (2011) considered numerically the effects of Brownian motion and thermophoresis of a nanofluid, on the boundary layer flow generated by a linearly stretching sheet with convective heating. They deduced that rising the local temperature thickens the thermal boundary layer as Brownian motion, thermophoresis and convective heating are each intensified.

A number of studies analyzing heat and mass transfer of nanofluids have been conducted (Kiblinki et al. 2002)-(Motsumi and Makinde 2012). Nevertheless, most of these studies did not put emphasis on the analysis pertaining to the combined effect of Couette flow, convective heat transfer and temperature dependant variable viscosity on the flow system. Furthermore, the study of is exceptionally crucial for innovative applications in hydrodynamic lubrication and cooling of engineering and industrial systems (Makinde and Onyejekwe 2011; Yasutomi et al. 1984).

In the present investigation, we have assumed that the flow is driven by the combined effects of pressure gradient and uniform velocity of the upper plate. The objective is to analysis the effect of variable viscosity on heat and mass transfer characteristics of Couette flow of nanofluids; taking into consideration, the Brownian motion of the particle and the effect of thermophoresis. The model used in this study is more general with regard to nanofluids and can be applied to any nanofluid flow without naming any nanoparticles involved. Semi-discretization technique was employed to solve the transient problem and the result

discretization was implemented using MATLAB.

## 2. MATHEMATICAL MODEL

Consider the unsteady laminar flow of an incompressible water base variable viscosity nanofluid between two parallel plates channel under the combined action of a constant pressure gradient and uniform motion of the upper plate. It is assumed that the channel width is  $a$ , the lower plate is fixed at  $y = 0$  ( $y$ -axis normal to the plate surface) while the upper plate uniform velocity is  $U$  as depicted in Fig. 1 below;

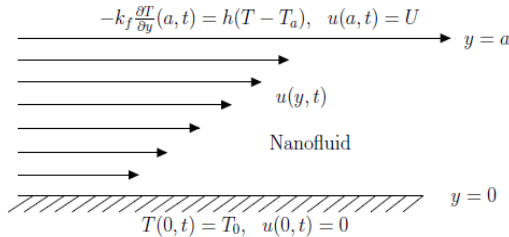


**Fig. 1. Schematic diagram of the problem under consideration.**

Using the Buongiorno (2006) nanofluid model with the Brownian motion, thermophoresis and nanoparticle volume fraction distributions, the governing equations for continuity, momentum, energy and nanoparticle concentration are

$$\frac{\partial u}{\partial x} = 0 \tag{1}$$

$$\rho_f \frac{\partial u}{\partial t} = -\frac{\partial P}{\partial x} + \frac{\partial}{\partial y} \left( \mu_f(T) \frac{\partial u}{\partial y} \right) \tag{2}$$

$$\begin{aligned} \frac{\partial T}{\partial t} = & \alpha_f \frac{\partial^2 T}{\partial y^2} + \frac{\alpha_f \mu_f(T)}{k_f} \left( \frac{\partial u}{\partial y} \right)^2 \\ & + \tau \left\{ D_B \frac{\partial T}{\partial y} \frac{\partial \phi}{\partial y} + \frac{D_T}{T_a} \left( \frac{\partial T}{\partial y} \right)^2 \right\} \end{aligned} \tag{3}$$

$$\frac{\partial \phi}{\partial t} = D_B \frac{\partial^2 \phi}{\partial y^2} + \left( \frac{D_T}{T_a} \right) \left( \frac{\partial^2 T}{\partial y^2} \right) \tag{4}$$

where  $D_B$  and  $D_T$  are the Brownian and thermophoretic diffusion coefficients respectively,  $u$  is the nanofluid velocity in the  $x$ -direction,  $T$  is the temperature of the nanofluid,  $P$  is the nanofluid pressure,  $t$  is the time,  $T_a$  is the ambient temperature,  $T_0$  is the nanofluid initial temperature which also correspond to the lower plate temperature,  $\phi$  is the concentration of nanoparticles,  $\rho_f$  is the density of the nanofluid,  $\alpha_f$  is the thermal diffusivity of the nanofluid and  $\tau$  is the ratio of solid particles heat capacitance to that of the nanofluid heat capacitance.

The dynamic viscosity of nanofluid is assumed to be temperature dependent as follows:

$$\mu_f(T) = \mu_0 e^{-m(T-T_0)} \tag{5}$$

where  $\mu_0$  is the nanofluid viscosity at the initial temperature  $T_0$  and  $m$  is the viscosity variation

parameter. The initial and boundary conditions are given as follows:

$$u(y, 0) = 0, T(y, 0) = T_0, \phi(y, 0) = \phi_0, \tag{6}$$

$$u(0, \bar{t}) = 0, T(0, \bar{t}) = T_0, \phi(0, \bar{t}) = \phi_0, \tag{7}$$

$$u(a, \bar{t}) = 0, -k_f \frac{\partial T}{\partial y}(a, \bar{t}) = h[T(a, \bar{t}) - T_a], \tag{8}$$

$$D_B \frac{\partial \phi}{\partial y}(a, \bar{t}) = -\frac{D_T}{T_a} \frac{\partial T}{\partial y}(a, \bar{t}),$$

where  $h$  is the heat transfer coefficient and  $\phi_0$  is the nanoparticles concentration at the lower plate which also corresponds to the initial nanoparticle concentration. We introduce the dimensionless variables and parameters as follows:

$$\theta = \frac{T - T_0}{T_a - T_0}, W = \frac{u}{U}, \eta = \frac{y}{a},$$

$$t = \frac{\bar{t}U}{a}, \nu_f = \frac{\mu_0}{\rho_f}, Bi = \frac{ha}{k_f},$$

$$\bar{P} = \frac{aP}{\mu_0 U}, Nb = \frac{\tau D_B \phi_0}{\alpha_f},$$

$$A = -\frac{\partial \bar{P}}{\partial X}, X = \frac{x}{a}, Pr = \frac{\mu_0 c_{pf}}{k_f}, \tag{9}$$

$$Ec = \frac{U^2}{c_{pf}(T_a - T_0)}, H = \frac{\phi}{\phi_0},$$

$$Nt = \frac{\tau D_T (T_a - T_0)}{\alpha_f T_a}, \tau = \frac{(\rho c_p)_s}{(\rho c_p)_f},$$

$$\beta = m(T_a - T_0), Sc = \frac{\nu_f}{D_B},$$

The dimensionless governing equations together with the appropriate initial and boundary conditions can be written as:

$$\frac{\partial W}{\partial t} = A + e^{-\beta \theta} \frac{\partial^2 W}{\partial \eta^2} - \beta e^{-\beta \theta} \frac{\partial \theta}{\partial \eta} \frac{\partial W}{\partial \eta} \tag{10}$$

$$\begin{aligned} Pr \frac{\partial \theta}{\partial t} = & \frac{\partial^2 \theta}{\partial \eta^2} + Ec Pr e^{-\beta \theta} \left( \frac{\partial W}{\partial \eta} \right)^2 \\ & + \left\{ Nb \frac{\partial \theta}{\partial \eta} \frac{\partial H}{\partial \eta} + Nt \left( \frac{\partial \theta}{\partial \eta} \right)^2 \right\} \end{aligned} \tag{11}$$

$$Sc \frac{\partial H}{\partial t} = \frac{\partial^2 H}{\partial \eta^2} + \frac{Nt}{Nb} \frac{\partial^2 \theta}{\partial \eta^2} \tag{12}$$

with

$$W(\eta, 0) = 0, \theta(\eta, 0) = 0, H(\eta, 0) = 1, \tag{13}$$

$$W(0, t) = 0, \theta(0, t) = 0, H(0, t) = 1, \tag{14}$$

$$W(1, t) = 1, \frac{\partial \theta}{\partial \eta}(1, t) = -Bi[\theta(1, t) - 1],$$

$$\frac{\partial H}{\partial \eta}(1, t) = -\frac{Nt}{Nb} \frac{\partial \theta}{\partial \eta}(1, t), \tag{15}$$

where  $Nb$  is the Brownian motion parameter,  $Nt$  is the thermophoresis parameter,  $Sc$  is the Schmidt number,  $Pr$  is the Prandtl number,  $Ec$  is the Eckert number,  $\beta$  is the viscosity variation parameter and  $A$  is the pressure gradient parameter.

The quantities of practical interest in this study are the skin friction coefficient  $C_f$  and the local Nusselt number  $Nu$  which are defined as

$$C_f = \frac{\tau_w}{\rho_f U^2}, \quad Nu = \frac{aq_w}{k_f(T_a - T_0)}, \quad (16)$$

where  $\tau_w$  is the shear stress and  $q_w$  is the heat flux at the upper moving plate given by

$$\tau_w = \mu_f \left. \frac{\partial u}{\partial y} \right|_{y=a}, \quad q_w = -k_f \left. \frac{\partial T}{\partial y} \right|_{y=a} \quad (17)$$

Substituting Eq. (17) into Eq. (16), we obtain

$$\left. \begin{aligned} Re_f C_f &= e^{-\beta\theta} \frac{\partial W}{\partial \eta}, \\ Nu &= -\frac{\partial \theta}{\partial \eta}, \end{aligned} \right\} \text{at } \eta = 1. \quad (18)$$

where  $Re_f = Ua/\nu_f$  is the flow Reynolds number.

### 3. NUMERICAL PROCEDURE

Equations (10)-(15) is clearly a system of nonlinear initial boundary value problem (IBVP) and can be solved numerically using a semi-discretization finite difference method known as method of lines (Na 1979).

The spatial interval  $0 \leq \eta \leq 1$  is partition into  $N$  equal parts and the grid size is given as  $\Delta\eta=1/N$  with the grid points  $\eta_i = (i-1)\Delta\eta$ ,  $1 \leq i \leq N+1$ . The discretization is based on a linear Cartesian mesh and uniform grid on which finite-differences are taken. The first and second spatial derivatives in Eqs.

(10)-(12) are approximated with second-order central finite differences. Let  $W_i(t)$ ,  $\theta_i(t)$  and  $H_i(t)$  be the approximation of  $W(\eta_i, t)$ ,  $\theta(\eta_i, t)$  and  $H(\eta_i, t)$ , then the semi-discrete system for the problem becomes

$$\frac{dW_i}{dt} = A + e^{-\beta\theta_i} \left( \frac{W_{i+1} - 2W_i + W_{i-1}}{\Delta\eta^2} \right) - \beta e^{-\beta\theta_i} \left( \frac{\theta_{i+1} - \theta_{i-1}}{2\Delta\eta} \right) \left( \frac{W_{i+1} - W_{i-1}}{2\Delta\eta} \right) \quad (19)$$

$$\begin{aligned} Pr \frac{d\theta_i}{dt} &= \frac{\theta_{i+1} - 2\theta_i + \theta_{i-1}}{\Delta\eta^2} + Nt \left( \frac{\theta_{i+1} - \theta_{i-1}}{2\Delta\eta} \right)^2 \\ &+ Nb \left( \frac{\theta_{i+1} - \theta_{i-1}}{2\Delta\eta} \right) \left( \frac{H_{i+1} - H_{i-1}}{2\Delta\eta} \right) \\ &+ EcPr e^{-\beta\theta_i} \left( \frac{W_{i+1} - W_{i-1}}{2\Delta\eta} \right)^2, \end{aligned} \quad (20)$$

$$\begin{aligned} Sc \frac{dH_i}{dt} &= \frac{H_{i+1} - 2H_i + H_{i-1}}{\Delta\eta^2} \\ &+ \frac{Nt}{Nb} \left( \frac{\theta_{i+1} - 2\theta_i + \theta_{i-1}}{\Delta\eta^2} \right), \end{aligned} \quad (21)$$

with initial conditions

$$W_i(0) = \theta_i(0) = 0, \quad H(0) = 1 \quad (22)$$

$1 \leq i \leq N + 1$

The equations corresponding to the first and last grid points are modified to incorporate the boundary conditions as follows

$$\begin{aligned} W_1 &= 0, \quad \theta_1 = 0, \quad H_1 = 1, \\ \theta_{N+1} &= \theta_N(1 - Bi\Delta\eta) + Bi\Delta\eta, \\ w_{N+1} &= 1, \quad H_{N+1} = H_N - \frac{Nt}{Nb}(\theta_{N+1} - \theta_N). \end{aligned} \quad (23)$$

We perform space discretize on Eq. (18) based on backward finite difference approximation and evaluate the results at  $\eta=1$  as follows

$$\begin{aligned} Re_f C_f &= \left( \frac{W_{N+1} - W_N}{\Delta\eta} \right) e^{-\beta\theta_{N+1}} \\ &= \frac{(1 - W_N) e^{-\beta[\theta_N(1 - Bi\Delta\eta) + Bi\Delta\eta]}}{\Delta\eta} \end{aligned} \quad (24)$$

Accordingly,

$$Nu = (\theta_N - 1)Bi \quad (25)$$

It is obvious that Eqs. (19)- (21) is a system of first order ordinary differential equations with known initial conditions and can be easily solved iteratively using Runge-Kutta Fehlberg integration technique Na (1979) implemented in computer using MATLAB. From the process of numerical computation, the skin-friction coefficient and the Nusselt number in Eq. (18) are obtained and their numerical values are presented.

### 4. RESULTS AND DISCUSSION

In this section, we present the results for the solution of the governing nonlinear initial and boundary value problem (IBVP). Numerical solution for the velocity field, temperature field, nanoparticle volume fraction, skin friction and Nusselt number have been carried out by assigning some specific values to various parameters controlling the flow system.

Unless otherwise stated, the values assigned to dimensionless parameters in this study are  $Pr=6.2$ ,  $Ec=1$ ,  $A=1$ ,  $Sc=1$ ,  $Nb=0.4$ ,  $Nt=0.16$ ,  $\beta=0.1$  and  $Bi=1$ . We have also taken space discretization size  $\Delta\eta$  0.005.

In the subsequent subsections, we discuss the transient flow and highlight the effects of various parameters on the nanofluid velocity, temperature and the nanoparticle volume fraction profiles as well as the skin friction and the local Nusselt number on the moving plate surface.

#### 4.1 Transient Flow

Figures 2-4 illustrate the evolutions of velocity, temperature and nanoparticle volume fraction profiles with the respect to the initial and boundary states of the flow system. Velocity increases from its zero value in time and space at the lower fixed plate to its maximum value at the upper moving plate before it reaches a steady state everywhere across the channel at around time  $t=0.5$  for the given set of parameter values.

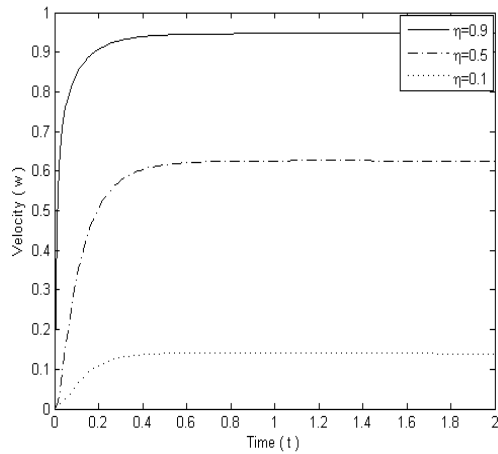


**Fig. 2. Velocity Evolution with Increasing  $\eta$ .**

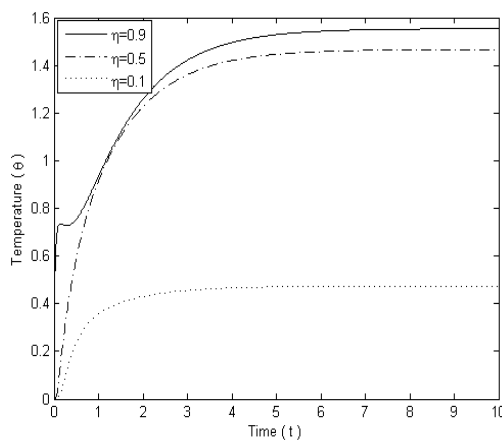


**Fig. 3. Temperature Evolution with Increasing  $\eta$ .**

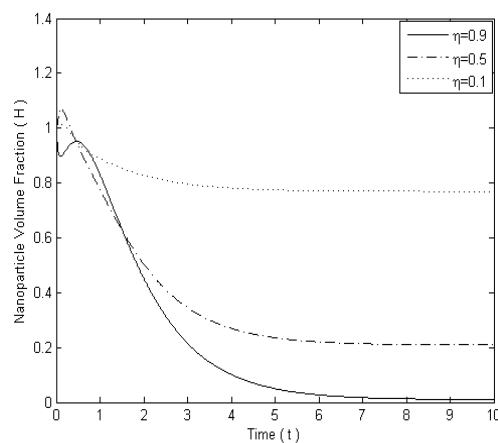


**Fig. 4. Nanoparticle Distr. Evolution with Increasing  $\eta$ .**

Similar trends are observed with temperature and nanoparticle volume fraction. It is worth noting that, around time  $t=10$ , all the three quantities had attained their steady states. The rest of the discussions are based on this time ( $t=10$ ). Relatively high concentration of nanoparticle is observed near the lower stationary plate, this is because of the prescribed boundary condition at the lower

stationary plate. Consequently, the temperature within the fluid near that upper moving plate becomes higher resulting in significant temperature drop near the lower plate. Whereas, near the upper moving plate, the nanoparticles concentration are relatively low. Hence, in spite of the presence of convective cooling from the ambient surroundings at the surface of the upper moving plate, the temperature is observed to be higher (see Figs. 3 and 4).

#### 4.2 Velocity Profiles with Parameter Variations.

In this Section, the velocity profiles are presented and effects of various parameters on the velocity are highlighted. Fig. 5 illustrates the velocity profile at three different instances.

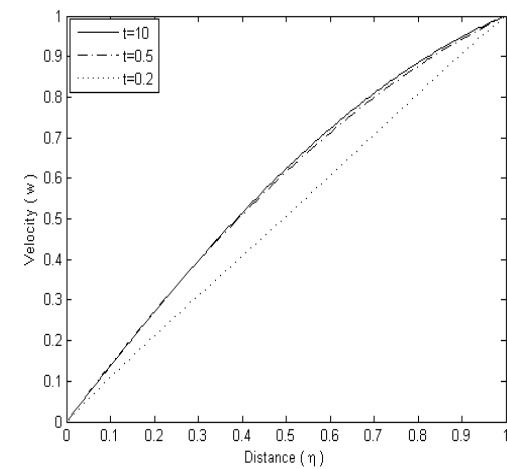


**Fig. 5. Velocity Profile with Increasing Time.**

It is observed that, the velocity grows gradually from its zero value at the lower stationary plate and acquire the maximum value at the moving upper plate satisfying the prescribed boundary conditions. It is also noticed that, the velocity tends to grow with time shortly before it stabilize. A selected set of graphical results presented in Figs. 6-7 gives a good insight of the influence of different parameters on the velocity profiles. The pressure gradient parameter  $A$  shows a significant effect on the velocity profile (see Fig. 6). As parameter  $A$  increased, the velocity increases. When set to  $A=0$ , the velocity takes a linear relationship with respect to channel width. In this case, the nanofluid is set in motion by the effect of the upper moving plate only. This was expected since Couette flow always exhibit linear relationship when pressure gradient is zero. The effect of variable viscosity parameter  $\beta$  is illustrated in Fig. 7. It can be observed that, increasing  $\beta$  reduces the fluid viscosity and hence, in turn, weaken the fluid resistance to flow. This invariably leads to an increase in the nanofluid velocity.

#### 4.3 Temperature Profiles with Parameter Variations

In this section, temperature profiles are illustrated

and effects of various parameters on temperature are discussed. Figure 8 presents the temperature profile across the channel with increasing time. Again, the temperature varies with time before it reaches a time where there is no further variation. At this stage we say, the temperature has attained its steady state.

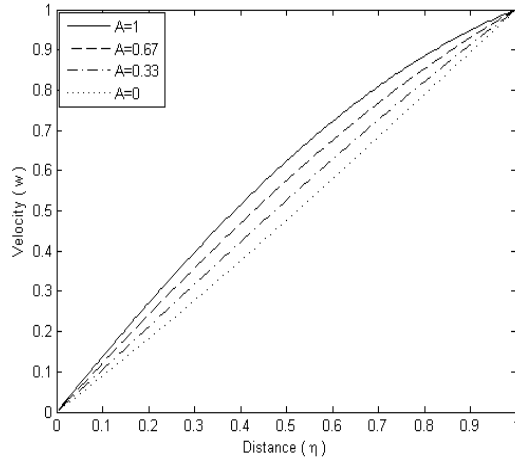


**Fig. 6. Effect of  $A$  on Velocity Profile.**

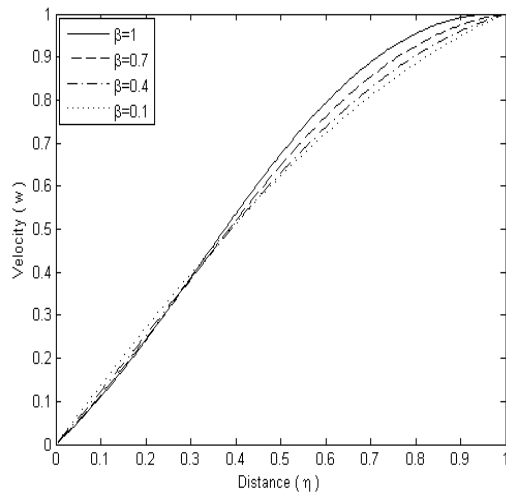


**Fig. 7. Effect of  $\beta$  on Velocity Profile.**

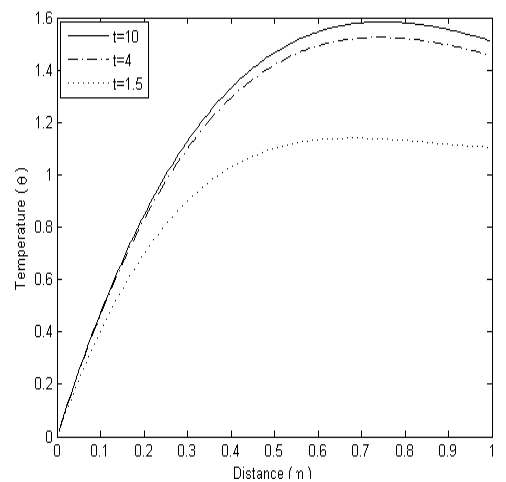


**Fig. 8. Temperature Profile with Increasing Time.**

When time is extended more we observe no changes in the temperature profile for a given set of parameter values. The effects of parameter variations on temperature profiles are highlighted in Figs. 9-11. The increased velocity due to the decrease in  $\beta$  boosts the viscous term in the temperature equation and hence increases the nanofluid temperatures as depicted in Fig. 9. The effects of the Biot number  $Bi$  on temperature profiles is illustrated in Fig. 10. It can be seen from the temperature boundary conditions given Eqs. (14)- (15) that, higher Biot number means higher level of convective cooling at the upper moving plate and hence the overall temperature profiles decrease with increasing Biot number. The reduced temperature increases the nanofluid flow resistance and hence decreases the nanofluid velocity.

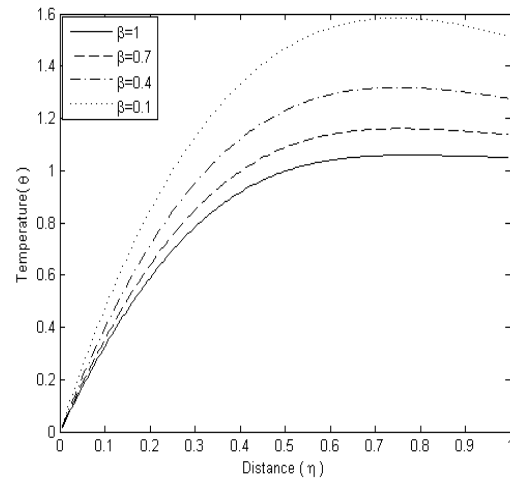


**Fig. 9. Effect of  $\beta$  on Temperature Profile.**

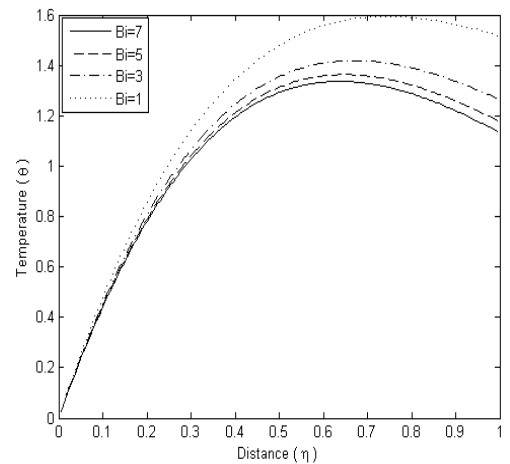


**Fig. 10. Effect of  $Bi$  on Temperature Profile.**

The effect of Eckert number  $Ec$  on temperature is depicted on Fig. 11. Accordingly, the increasing  $Ec$  causes the temperature profile to rise as well. This may be attributed to an increase in internal viscous heating of nanofluid.

#### 4.4 Nanoparticles Concentration with Parameter Variations

The nanoparticles concentration profiles are

discussed in this section. Fig. 12 shows the nanoparticles concentration profiles across the channel with increasing time. The particles decrease with time before reaching a steady state. The nanoparticles concentration is kept constant at the lower stationary plate. Figs. 13-17 demonstrate the effects of various parameters on nanoparticles concentration.

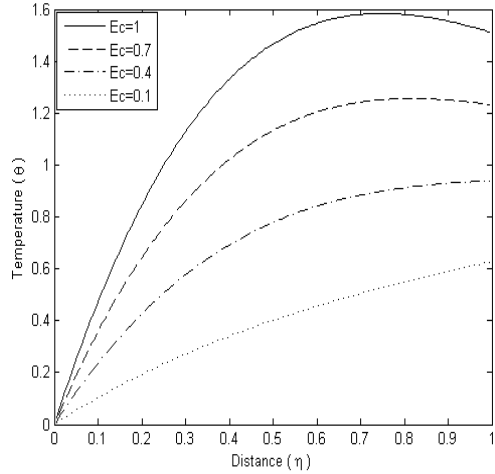


**Fig. 11. Effect of  $Ec$  on Temperature Profile.**

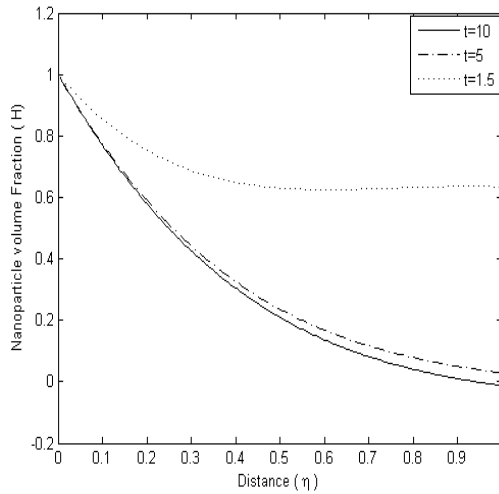


**Fig. 12. Nanoparticle Distr. Profile with Increasing Time.**

The effect of Brownian motion parameter  $Nb$  is shown in Fig. 13. It is observed that nanoparticles concentration rises with the increase in  $Nb$  while  $Nt$  is fixed at  $Nt = 0.1$ . Opposite behavior is observed when the thermophoresis parameter  $Nt$  is varied (see Fig. 14).

The effects of the Biot number  $Bi$  on nanoparticles concentration profiles is illustrated in Fig. 15 with  $Nt = 0.1$ . We notice that, an increase in  $Bi$  tends to lower the nanoparticles concentration, consequently diminishes the growth of temperature across the channel which would have been produced due to the thermophoretic friction among the particles.

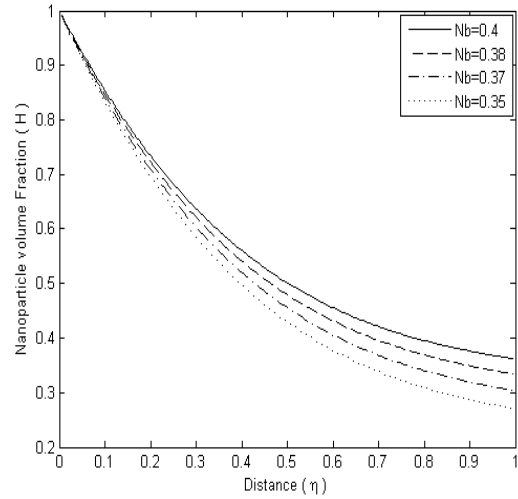


**Fig. 13. Effect of  $Nb$  on Nanoparticle Distr. Profile.**

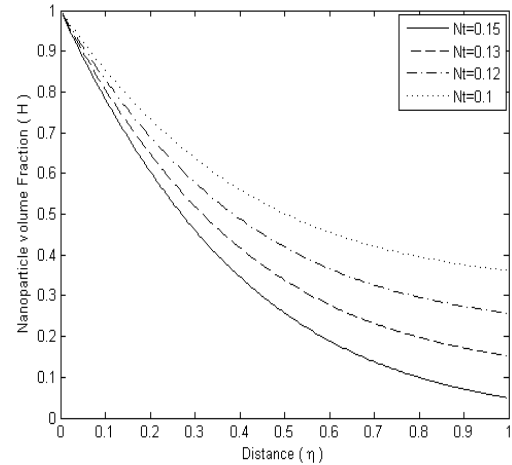


**Fig. 14. Effect of  $Nt$  on Nanoparticle Distr. Profile.**

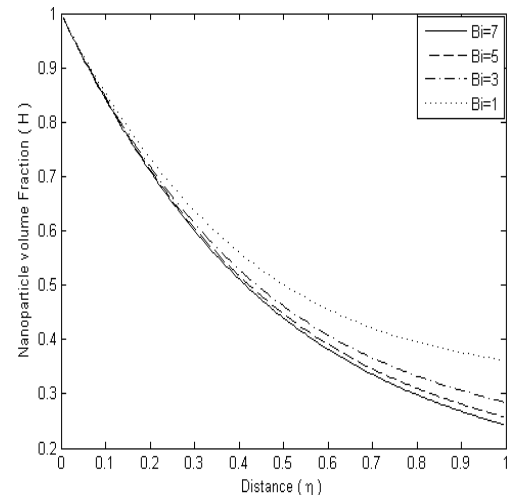


**Fig. 15. Effect of  $Bi$  on Nanoparticle Distr. Profile.**

The effect of Schmidt number  $Sc$  is presented in Fig. 16. Increase in  $Sc$  increases nanoparticles concentration at the lower fixed plate but decreases the concentration at the upper moving plate.

**Table 1 Nusselt Number and Skin Friction with Parameters Variations.  $Pr = 6.2, Sc = 1$**

Time	Parameters						$Re_f C_f$	$Nu$
	$A$	$Ec$	$Nt$	$Bi$	$\beta$	$Nb$		
0.1	1.0	1.0	0.16	1	0.1	0.40	1.405	-0.184
1.0	1.0	1.0	0.16	1	0.1	0.40	0.434	-0.063
6.0	1.0	1.0	0.16	1	0.1	0.40	0.397	0.502
9.5	1.0	1.0	0.16	1	0.1	0.40	0.397	0.512
10	1.0	1.0	0.16	1	0.1	0.40	0.397	0.512
10	0.5	1.0	0.16	1	0.1	0.40	0.638	0.641
10	0.0	1.0	0.16	1	0.1	0.40	0.875	0.826
10	1.0	0.5	0.16	1	0.1	0.40	0.435	0.039
10	1.0	0.1	0.16	1	0.1	0.40	0.471	-0.374
10	1.0	1.0	0.13	1	0.1	0.40	0.396	0.516
10	1.0	1.0	0.10	1	0.1	0.40	0.396	0.519
10	1.0	1.0	0.16	3	0.1	0.40	0.406	0.790
10	1.0	1.0	0.16	7	0.1	0.40	0.411	0.943
10	1.0	1.0	0.16	1	0.5	0.40	0.145	0.223
10	1.0	1.0	0.16	1	1.0	0.40	-0.018	0.050
10	1.0	1.0	0.10	1	0.1	0.37	0.396	0.519
10	1.0	1.0	0.10	1	0.1	0.35	0.396	0.519

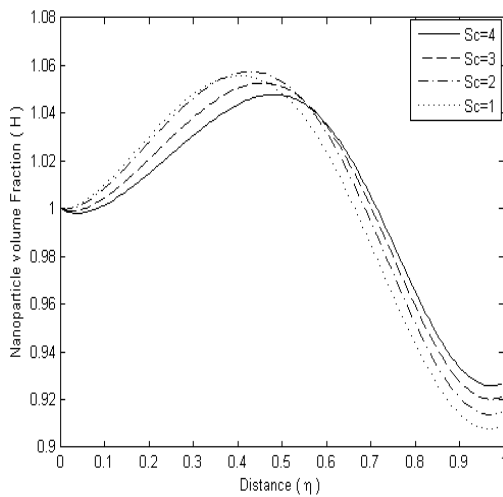


**Fig. 16. Effect of  $Sc$  on Nanoparticle Distr. Profile.**

Moreover, it is noteworthy from Eq. (12) that no effect of  $Sc$  will be observed at steady state. Fig. 17 shows increase in the nanoparticles concentration with increasing values of pressure gradient  $A$ . This is because more nanoparticles are taken in the flow stream when the pressure gradient is raised.

**4.5 Skin Friction and Nusselt Number Profiles**

Table 1 presents the variation in the skin friction and Nusselt number for different values of pressure gradient parameter, Biot number, Brownian motion parameter, Eckert number, variable viscosity and thermophoresis parameters. Skin friction is observed to decrease while the Nusselt number increases with time before attaining their steady values at about time  $t = 10$ . We also noticed that as  $Bi$  increases, both the skin friction and Nusselt number increase. This is so because when  $Bi$  is increased, the temperature in the system is lowered and therefore the heat transfer rate ( $Nu$ ) is increased and the skin friction becomes higher because rise in

viscosity when the temperature is lowered. Opposite behavior with a decrease in skin friction and Nusselt number are observed when pressure gradient parameter  $A$  and variable viscosity parameter  $\beta$  are increased. Very little effects are observed when  $Nt$  and  $Nb$  is changed. Furthermore, the skin friction decreases while the Nusselt number increases with an increase in Eckert number  $Ec$ .

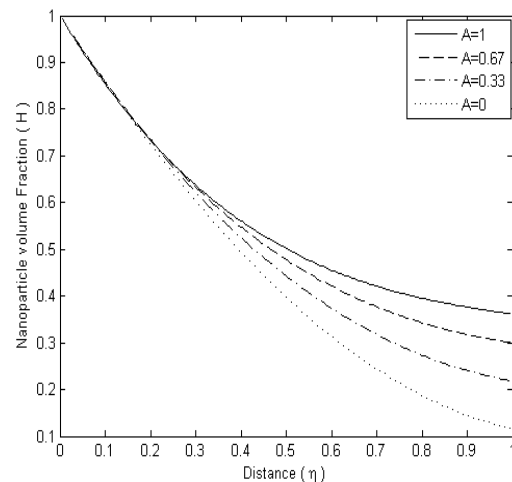


**Fig. 17. Effect of  $A$  on Nanoparticle Distr. Profile.**

Figures 18-19 present the skin friction and Nusselt number profiles. The skin friction is plotted against  $\beta$  while varying the  $Bi$ , and Nusselt number is plotted against the  $Bi$  while varying  $\beta$ . It can be observed that the skin friction decreases with increase in  $\beta$  and increases with  $Bi$  while the Nusselt number increases with both  $\beta$  and  $Bi$ .

**5. CONCLUSION**

In this work, the effects of temperature dependan

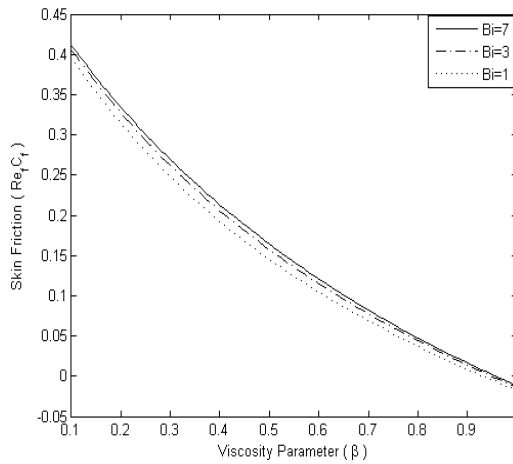


**Fig. 18. Skin Friction Profile.**

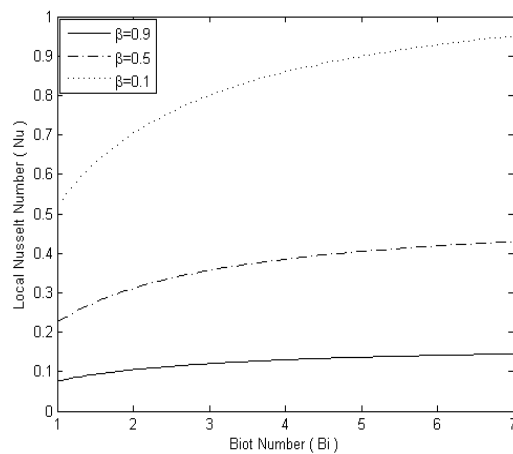


**Fig. 19. Nusselt Number Profile.**

$t$  variable viscosity on the Couette flow of water based nanofluid, with convective cooling at the moving plate were analyzed, with regards to heat and mass transfer in the system, taking into consideration the Brownian motion and thermophoresis. Numerical procedures were sought to solve the governing equations of the proposed system. The following is the summary drawn from the overall analysis.

- Velocity and temperature profiles evolved with time from zero initial values before attaining their steady state values. The nanoparticle volume fraction dropped from its unity initial value and reached steady state in the long run.
- While other parameter remain unchanged, the velocity profile increases with the increase of  $A$  or variable viscosity parameter  $\beta$ . Temperature decrease with the increase of  $\beta$  (increasing  $\beta$  decrease viscosity) or  $Bi$  with other parameters remain unchanged.
- Rising  $Ec$  causes cause temperature profile to rise while demonstrating little effect on both velocity and particle volume distribution profile.
- Variation of Schmidt number  $Sc$  shows significant effect on the nanoparticle volume distribution profile before the system reached steady state, and demonstrates no effect at all

when the system attained steady state.

- $Nb$  reduce the rate of decrease of nanoparticle volume fraction distribution while  $Nt$  shown the reverse effect.
- Skin friction increase with the increase of viscosity (decreasing  $\beta$ ).
- The local Nusselt number and (hence convective cooling) increases with the increase in  $Bi$ .

#### ACKNOWLEDGEMENTS.

Authors would like to thank The Nelson Mandela African Institution of Science and Technology for financial support and the anonymous reviewers for their invaluable comments.

#### CONFLICT OF INTEREST.

The authors declare that there is no conflict of interest to disclose.

#### REFERENCES

- Asghar, S. and A. Ahmad (2012). Unsteady Couette flow of viscous fluid under a non-uniform magnetic field. *Applied Mathematics Letters* 25(11), 1953-1958.
- Buongiorno, J. (2006). Convective transport in nanofluids. *Journal of Heat Transfer* 128(3), 240-250.
- Chinyoka, T. and O. D. Makinde (2011). Analysis of transient generalized Couette flow of a reactive variable viscosity third-grade liquid with asymmetric convective cooling. *Mathematical and Computer Modelling* 54(1), 160-174.
- Choi, S. U. S. (1995). Enhancing thermal conductivity of fluids with nanoparticles. In Singer, D and Wang, H (Eds.), *Development and Applications of Non-Newtonian Flows*, American Society of Mechanical Engineers, New York, 99-106.
- Choi, S., Z. Zhang, W. Yu, F. Lockwood and E. Grulke (2001). Anomalous thermal conductivity enhancement in nanotube suspensions. *Applied Physics Letters* 79(14), 2252-2254.
- Das, S., S. Maji, M. Guria and R. Jana (2009). Unsteady MHD Couette flow in a rotating system. *Mathematical and Computer Modelling* 50(7), 1211-1217.
- Dong, L. and D. Johnson (2005). Experimental and theoretical study of the interfacial instability between two shear fluids in a channel Couette flow. *International Journal of Heat and Fluid Flow* 26(1), 133-140.

- Eastman, J. A., S. Phillpot, S. Choi and P. Keblinski (2004). Thermal transport in nanofluids 1. *Annu. Rev. Mater. Res.* 34, 219-246.
- Gireesha, B., A. Chamkha, C. Vishalakshi and C. Bagewadi (2012). Three-dimensional Couette flow of a dusty fluid with heat transfer. *Applied Mathematical Modelling* 36(2), 683-701.
- Kakac, S. and A. Pramuanjaroenkij (2009). Review of convective heat transfer enhancement with nanofluids. *International Journal of Heat and Mass Transfer* 52(13), 3187-3196.
- Kiblinki, P., S. R. Phillpot, S. U. S. Choi and J.A. Eastman (2002). Mechanism of heat flow suspensions of nano-sized particles (nanofluids). *International Journal of Heat and Mass Transfer* 42, 855-866.
- Gao, P. and X. Y. Lu (2013). On the wetting dynamics in a Couette flow. *Journal of Fluid Mechanics* 724, R1.
- Hatami, M., M. Sheikholeslami and G. Domairry (2014). High accuracy analysis for motion of a spherical particle in plane Couette fluid flow by Multi-step Differential Transformation Method. *Powder Technology* 260, 59-67.
- Jamai, H., S. O. Fakhreddine and H. Sammouda (2014). Numerical study of sinusoidal Temperature in magneto-convection *Journal of Applied Fluid Mechanics* 7(3), 493-502.
- Kuznetsov, A. V. and D. A. Nield (2014). Natural convective boundary-layer flow of a nanofluid past a vertical plate: A revised model. *International Journal of Thermal Sciences* 77, 126-129.
- Maiga, S. E. B., S. J. Palm, C. T. Nguyen, G. Roy and N. Galanis (2005). Heat transfer enhancement by using nanofluids in forced convection flows. *International Journal of Heat and Fluid Flow* 26(4), 530-546.
- Makinde, O. D. and A. Aziz (2011). Boundary layer flow of a nanofluid past a stretching sheet with a convective boundary condition. *International Journal of Thermal Sciences* 50(7), 1326-1332.
- Makinde, O. D. (2004). Effects of viscous dissipation and Newtonian heating on boundary-layer flow of nanofluids over a plate. *International Journal of Numerical Methods for Heat and Fluid Flow* 23(8), 1291-1303.
- Makinde, O. D. and O. Onyejekwe (2011). A numerical study of MHD generalized Couette flow and heat transfer with variable viscosity and electrical conductivity. *Journal of Magnetism and Magnetic Materials* 323(22), 2757-2763.
- Motsumi, T. and O. D. Makinde (2012). Effects of thermal radiation and viscous dissipation on boundary layer flow of nanofluids over a permeable moving at plate. *Physica Scripta* 86(4), 045003.
- Na, T. Y. (1979). *Computational methods in engineering boundary value problems*. Vol. 220. New York: Academic Press.
- Nag, S., Jana, R. and N. Datta (1979). Couette flow of a dusty gas *Acta Mechanica* 33(3), 179-187.
- Sheikholeslami, M., M. Gorji-Bandpy and G. Domairry (2013). Free convection of nanofluid filled enclosure using lattice Boltzmann method (LBM). *Applied Mathematics and Mechanics* 34(7), 833-846.
- Sheikholeslami, M. and D. D. Ganji (2014). Heated permeable stretching surface in a porous medium using Nanofluids. *Journal of Applied Fluid Mechanics* 7(3), 535-542.
- Trisaksri, V. and S. Wongwises (2007). Critical review of heat transfer characteristics of nanofluids. *Renewable and Sustainable Energy Reviews* 11(3), 512-523.
- Wang, X. and A. S. Mujumdar (2007). Heat transfer characteristics of nanofluids: a review. *International Journal of Thermal Sciences* 46(1), 1-19.
- Wang, X., Xu, X. and S. U. S. Choi (1999). Thermal conductivity of nanoparticle-fluid mixture. *Journal of Thermophysics and Heat Transfer* 13(4), 474-480.
- Xuan, Y. and W. Roetzel (2000). Conceptions for heat transfer correlation of nanofluids. *International Journal of Heat and Mass Transfer* 43(19), 3701-3707.
- Yasutomi, S., S. Bair and W. Winer (1984). An application of a free volume model to lubricant rheology independence of viscosity on temperature and pressure. *Journal of Tribology* 106(2), 291-30